Towards a better understanding of structure-performance relation in PEMFC fuel cells based on ptychography X-ray nanotomography and

Towards a better understanding of structure-performance relation in PEMFC fuel cells based on ptychography X-ray nanotomography and scanning small angle X-ray scattering

C. Appel[1], K. Jeschonek[2], K. Brunnengräber[2], B. J. M. Etzold[2], M. Liebi[3,4], M. Guizar-Sicairos[1]

[1] Paul Scherrer Institut (PSI), CH-5232 Villigen PSI, Switzerland, [2] Technical University of Darmstadt, Darmstadt-64287, Germany,

[3] EMPA – Center of X-ray analytics, St. Gallen-9014 Switzerland, [4]Chalmers University of Technology, Gothenburg 41296, Sweden

Motivation

- Gaining fundamental insights on the structure of advanced composite materials is challenging, but essential for their role in respect to future energy challenges
- This project explores the possibility to combine high resolution imaging with coherent X-rays (Ptychographic X-ray Tomography - PXCT) together with SAXS (small angle X-ray scattering) imaging to obtain full scale models on multiple length scales (nano- to millimetre)
- The analysis approach is complemented by additional methods such as X-ray fluorescence performed simultaneously to SAXS imaging

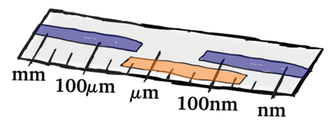

Methods

Ptychography X-ray Tomography

- PXCT measures far-field diffraction patterns from a sample that is moved across a spatially confined coherent beam in a way that illumination areas overlap. This is carried out for multiple sample orientations
- An iterative phase retrieval algorithm together with a tomography reconstruction is able to reconstruct the electron density (ED) distribution in 3D
- Samples were measured under cryo-conditions with OMNY[1] at 6.2keV; 25-40μm sample diameter; 3D half-period resolution of 24-34nm estimated by Fourier shell correlation

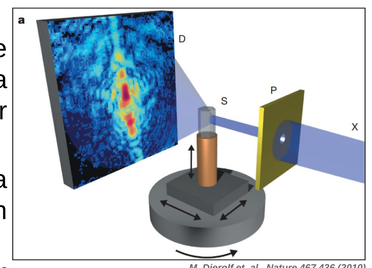

M. Dierolf et. al., Nature 467 436 (2010)

2D SAXS & XRF imaging

- Scanning SAXS measurement at 11.2keV were performed with a local resolution of 10μm, scanning 1x1mm² for all 3 catalysts at two sample-detector distances (2m & 7m)
- X-ray fluorescence was collected simultaneously to complement the scattering data at each position

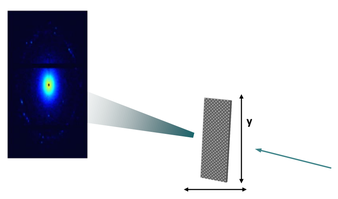

Materials and electrochemical performance

Polymer electrolyte membrane fuel cells (PEMFCs) generate electricity by electrochemical reaction that take place in a complex porous material (catalyst layer) with 3 components

Catalyst layer sprayed on Nafion[221]

Three components:

1.) Support: Carbon (Vulcan XC72R)

2.) Binder: Ionomer (Nafion)

3.) Active sites: Pt nanoparticle (~3-4nm)

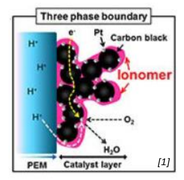

Samples with three different Ionomer/Carbon (I/C) ratios:

	Pt / wt%	Ionom. wt%	Carbon wt%	SLD [10^{-6}Å^{-2}]
I/C 0.2	16.8	13.8	67.4	39.1
I/C 0.54	13.6	30.5	52.9	34.8
I/C 0.95	11.1	43.2	45.7	31.5
ED [e/Å³]	5.167	0.593 (dry)	0.57-0.63	

[1] http://www.jaist.ac.jp/ms/labs/nagao-www/wp-content/uploads/2018/07/20180704labguide2018.pdf

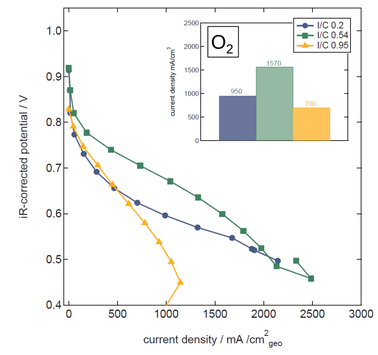

Flow: 0.2 L/min H_2 and O_2; 100%RH; OCV vs 0.3V; 80°C 5cm² cell

Results

- Isotropic scattering
- Data merged from three detectors
- Catalyst sprayed on Nafion[221]

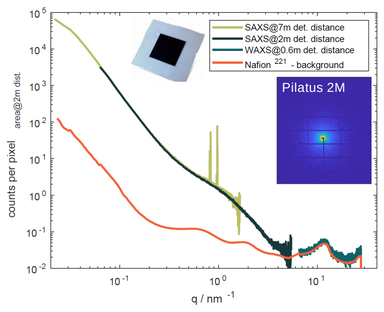

- Absolute scattering
- Q-invariant analysis, assuming two phase system

$$Q = \int_0^\infty q^2 \, (I_{abs}(q) - I_{bkg}(q)) \, dq$$

$$\phi_1 \phi_2 = \frac{Q}{2\pi^2 (\Delta\rho_{SLD})^2}$$

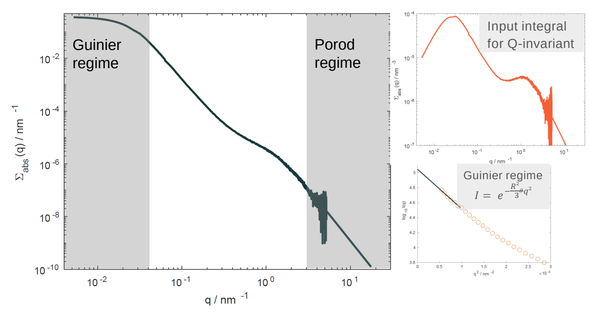

- XRF spectra
- 3 Pt and S line at 2…2.3keV overlap
- Peaks fitted by linear combination of pure materials

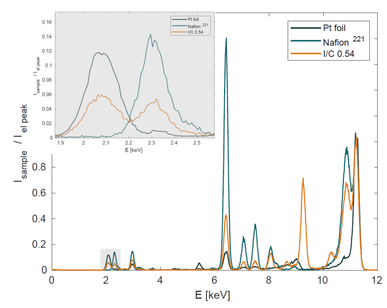

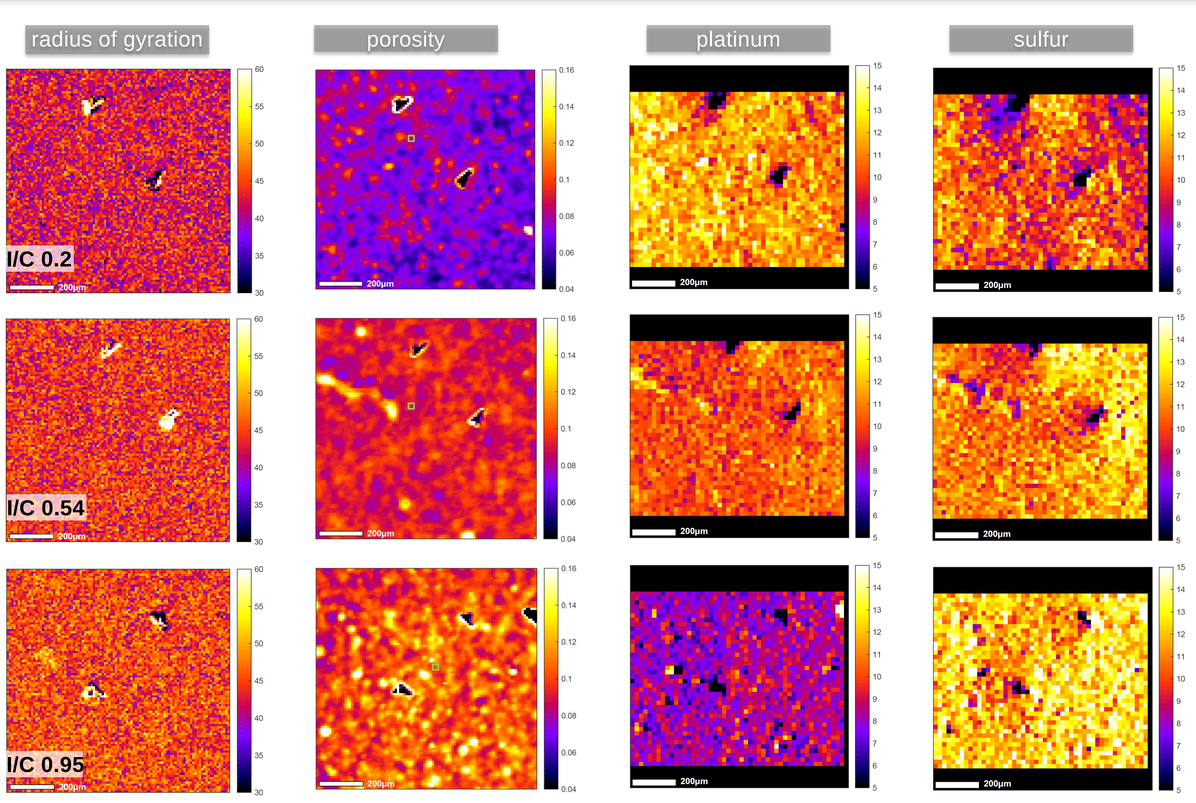

μm-pillars & ED PXCT reconstructions

2D tomography slices (xz, bottom & xy, right) for ED reconstructions

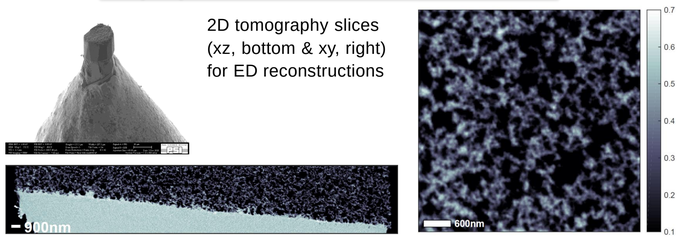

Performance wise, best material

μ-pillar position highlighted in porosity map □

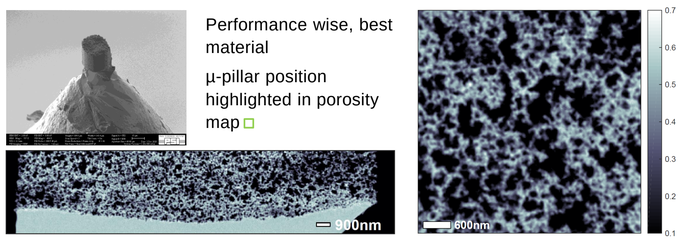

Highest ionomer concentration

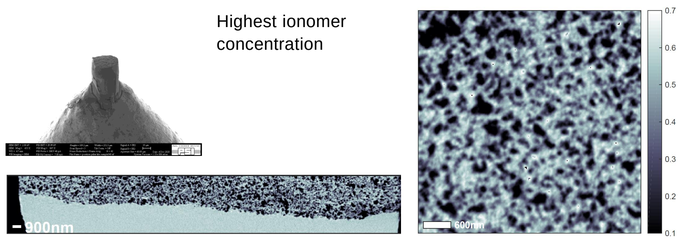

segmented pore network

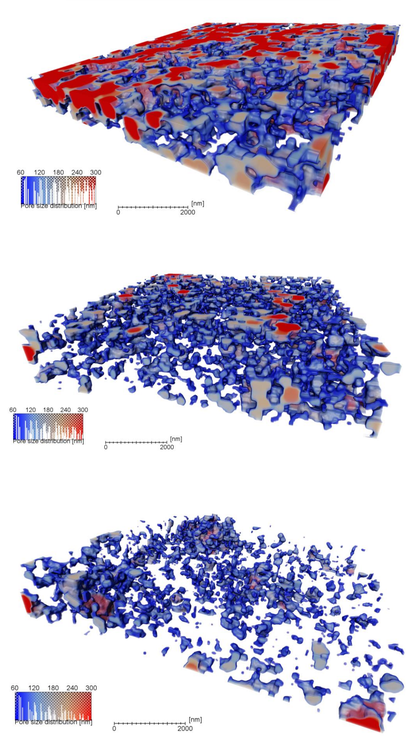

Compare and discuss results

XRF maps

- Amplitude histogram for both elements show the expected increase in S with increasing ionomer concentration.
- Pt peaks do not overlap, contrary to expectation, however sample self-absorption correction is still missing which may solve this

Pore size distribution

- Pore size distribution is segmented for all samples from PXCT by threshold segmentation (ED < 0.1 Å^{-3})
- Radius of gyration, assuming spherical shape, matches well with the smallest pore size accumulation of PXCT distributions

Pore volume fraction (PVF)

- PVF for full PXCT is quite different from SAXS results
- SAXS picks up pores from 1…100nm (q-resolution) and agrees with results for small pores < 120nm PVF (PXCT) quite good
- PVF from all pores shows strong increase for I/O 0.2 (good performing) & I/O 0.54 (best performance), missing feature for I/C 0.95 (worst performance) catalyst layer

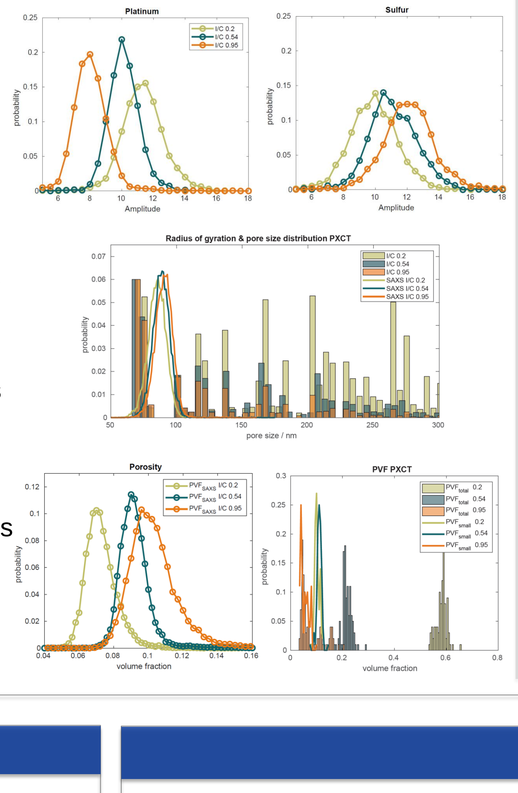

Outlook

- SAXS: Full q-range modelling of data, morphological model for micropores and additionally feed models with DFT results from Ar gas adsorption results
- XRF: Correct Pt & S amplitudes by sample self-absorption
- PXCT: Gradient based segmentation for pores, support and ionomer
- Modelling: Use SAXS, XRF & PXCT results to generate 3D models based on elemental distribution, pore volume fraction and pore size distribution

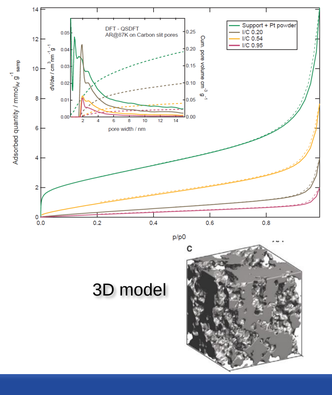

3D model

Summary

- SAXS & PXCT provide data on different length scales, but with a well resolved overlap
- SAXS & XRF maps show homogeneous layers on macroscopic. length scales (μm to mm)
- Element distribution as expected from chemical composition
- Pore volume fraction indicates that large pore network may be responsible for performance decrease of I/C 0.95 (mass diffusion limitations); PXCT ED reconstruction also show dense electron density

References

[1] M. Holler, M. Guizar-Sicairos, et. Al. (2017). *Rev. Sci. Instrum.* 88(11),113701.

[2] A. Rodriguez-Palomo, M. Liebi, et. Al. (2021). *Small.* 17, 2006229.

[3] C. Gommes et. Al. (2019). *Journal of Applied Crystallography.* 52, 507-519.

Acknowledgement

This project has received funding from the European Union's Horizon 2020 research and innovation program under the Marie Sklodowska-Curie grant agreement No. 701647 (PSI-FELLOW-III-3i), from the European Research Council (ERC) grant agreement No. 681719, and funding from the Chalmers initiative for advancement of neutron and X-ray techniques. The authors also acknowledge the Paul Scherrer Institut, Villigen, Switzerland for provision of synchrotron radiation beamtime at beamline cSAXS of the SLS.